JOURNAL OF GEOPHYSICAL RESEARCH, VOL. 109, D20308, doi:10.1029/2004JD004677, 2004

Long-term global measurements of ozone profiles by GOME validated with SAGE II considering atmospheric dynamics

A. Bracher, M. Weber, K. Bramstedt, S. Tellmann, and J. P. Burrows
Institute of Environmental Physics, University of Bremen, Bremen, Germany

Received 23 February 2004; revised 18 August 2004; accepted 24 August 2004; published 29 October 2004.

[1] Stratospheric ozone profiles measured by the Global Ozone Monitoring Experiment (GOME on ERS-2) and Stratospheric Aerosol and Gas Experiment II (SAGE II on ERBS, data version 6.2) were compared over a 4-year time period (1996–2000). GOME measures the reflected and backscattered radiation from Earth, and vertical profiles are derived from nadir observations using the Full Retrieval Method (FURM, version 5.0), which is based upon an advanced optimal estimation inversion scheme; SAGE II uses solar occultation to measure vertical profiles of ozone with an instantaneous vertical field of view of 0.5 km at the Earth limb. Coincident measurements are identified by limiting time differences and distance between two observation points. Since for ozone in the lower stratosphere gradients in the horizontal distribution evolve from transport processes, validation at the border of different air masses is rendered more difficult. Important factors influencing the ozone distribution are the tropopause height and whether a measurement is taken within or outside the polar vortex. This was taken into account when the validation was reduced to matches where both measurements were within the same air mass. Overall, comparisons show that between 19- and ~34-km good agreement between the ozone profiles of the two satellite instruments is achieved. If lower stratospheric ozone is strongly depleted during polar spring, a homogeneity condition has to be imposed on the GOME and SAGE II measurements by requiring an upper limit on the potential vorticity difference at the 475-K isentrope. *INDEX TERMS:* 0340 Atmospheric Composition and Structure: Middle atmosphere—composition and chemistry; 3334 Meteorology and Atmospheric Dynamics: Middle atmosphere dynamics (0341, 0342); 3362 Meteorology and Atmospheric Dynamics: Stratosphere/troposphere interactions; 3360 Meteorology and Atmospheric Dynamics: Remote sensing; *KEYWORDS:* ozone profiles, GOME, SAGE II

Citation: Bracher, A., M. Weber, K. Bramstedt, S. Tellmann, and J. P. Burrows (2004), Long-term global measurements of ozone profiles by GOME validated with SAGE II considering atmospheric dynamics, *J. Geophys. Res.*, *109*, D20308, doi:10.1029/2004JD004677.

1. Introduction

[2] Atmospheric ozone plays an important role in the Earth's radiation budget because it absorbs both short-wave and long-wave radiation [*Ramanathan et al.*, 1976; *Ramanathan and Dickinson*, 1979; *Fishman et al.*, 1979]. Decreases of stratospheric ozone in middle and high latitudes, resulting from anthropogenic emissions of chlorofluorocarbons (CFC), cool the surface, while increase of surface and upper tropospheric ozone from photochemical production increases the surface temperature. The overall effect of ozone on climate is highly sensitive not only to its amount but also to its vertical distribution [*Wang et al.*, 1993]. Understanding the cause of observed negative trends in the column requires knowledge of the changing shape of the ozone profile. Long-term observations of the ozone profile are needed to assess the current behavior and potential future changes.

0148-0227/04/2004JD004677$09.00

[3] With the development of satellite-borne sensors, stratospheric ozone measurements can be extended to near-global coverage. It is particularly important that satellite measurements of stratospheric ozone be routinely compared with independent measurements to verify the long-term stability of the instrument performance. As satellite instruments age and unfortunately die, it is necessary to compare the ozone measurements from older instruments with those from newer instruments in order to ensure that long-term behavior, derived from a combination of ozone sensors, will be useful [e.g., *Cunnold et al.*, 1996].

[4] The Global Ozone Monitoring Experiment (GOME) is a UV/VIS grating spectrometer aboard the ERS-2 satellite, which was launched in April 1995 [*Burrows et al.*, 1999]. GOME measures the reflected and backscattered radiation from Earth. Vertical profiles are derived from nadir observations using the Full Retrieval Method (FURM), which is based upon an advanced optimal estimation inversion scheme [*de Beek et al.*, 1997; *Hoogen et al.*, 1999a]. The longest record of satellite high-resolution

profile measurements has been made by the solar occultation instrument Stratospheric Aerosol and Gas Experiment (SAGE II), which was launched on the Earth Radiation Budget Satellite (ERBS) in October 1984 and is still operational and collecting data. Compared to GOME, which is a nadir-viewing instrument and covers the entire surface within 3 days, the solar occultation instrument SAGE II has a repeat cycle of slightly more than a month. On the other hand, SAGE II pixel size is smaller, and the vertical resolution is higher than that of the profiles retrieved from GOME. In addition to that, data from the SAGE II instrument have been extensively validated, and the accuracy of the previous SAGE II ozone profile version 6.1 is documented to be within 5% between 15 and 50 km [*Wang et al.*, 2002]. Thus comparisons of ozone profiles from SAGE II and GOME provide a unique opportunity to validate the GOME data products. As both instruments have been operated concurrently for a sufficiently long period, the long-term behavior and zonal characteristics can be analyzed and compared.

[5] For long-lived substances, such as ozone in the lower stratosphere, validation at the edge of different air masses is more difficult, because gradients in the horizontal distribution result from transport processes. At the potential temperature of 475 K (~19 km altitude) there is a strong gradient in potential vorticity range between 30 and 40 PVU in the Northern Hemisphere and −40 to −30 PVU in the Southern Hemisphere. These PV values indicate the edge of the polar vortices, which separate low ozone concentrations inside the polar vortex from high ozone concentrations outside the polar vortex. At the 475 K isentrope, ozone destruction within the polar vortex maximizes, and therefore differences in ozone concentration are most pronounced at this isentropic level. Studies by *Weiss* [2000] on long-term measurements of ozonesondes showed that more than half of the ozone variability in the midlatitudes can be explained by a linear dependence between total ozone and tropopause height; additional factors are chemical ozone loss, the amount of stratospheric aerosols from massive volcano eruptions, and the solar variability. *Eichmann* [2001] showed that an increase of the tropopause height by 1 km in extratropical regions corresponds to a decrease of 40–50 DU. At high tropopause heights the ozone concentration can be reduced up to the isentropic level of around 550 K [*Zellner et al.*, 1999]. In this context the appearance of ozone miniholes is significant. These result from large horizontal divergent transport of ozone from the lower stratospheric layer above a high tropopause, which rapidly reduces the total column in a localized region [e.g., *Newman et al.*, 1988; *McKenna et al.*, 1989; *James*, 1998; *Eichmann et al.*, 1999, 2000; *Weber et al.*, 2002]. Besides identifying collocated measurements by limiting time difference and distance between two observation points, additional criteria were selected to ensure that observations were made in the same air masses. The tropopause height and the position of the polar vortex were determined by analysis of the potential vorticity (PV) distribution.

[6] This study presents the comparison of coincident ozone profiles retrieved from GOME nadir measurements and SAGE II occultation measurements over a 4-year period including statistical analyses. Thereby, zonal and dynamical aspects have been explicitly considered and provide insight into the data quality of the measurements.

2. Instruments and Data Analysis

2.1. Instrument Description and Retrieval Methods

2.1.1. GOME

[7] The nadir-viewing instrument GOME on board ERS-2 measures the radiation scattered back or reflected from the Earth and its atmosphere. ERS-2 flies in a Sun-synchronous near-polar orbit at a mean altitude of 795 km. The equator-crossing time in the descending node is at 1030 local time (LT). Global coverage is achieved after 42 orbits or approximately 3 days. At latitudes higher than 65°, complete coverage is provided daily except for the polar night region. Measurements cover the entire spectrum from 240 nm to 790 nm with a spectral resolution varying between 0.2 and 0.3 nm and are taken within four separate spectral channels [*Burrows et al.*, 1999]. The measurement sequence of an across scan lasts 6 s; three radiance measurements are taken in 1.5 s in the forward direction covering, together, a maximum surface area of 40 km × 960 km and the final back scan.

[8] The short-wave region of GOME covers the Hartley-Huggins ozone bands, which contain information about the vertical ozone distribution. The retrieval algorithm Full Retrieval Method (FURM) has been developed to derive ozone profiles from the UV/VIS spectral range [*de Beek et al.*, 1997; *Hoogen et al.*, 1999a]. FURM consists of two major parts: first, a forward model, the pseudospherical multiple-scattering radiative transfer model GOMETRAN [*Rozanov et al.*, 1997], calculating the top-of-atmosphere (TOA) radiance for a given state of the atmosphere; second, an iterative inversion scheme that adjusts this state to match that calculated with the measured TOA radiance, utilizing the so-called weighting functions also provided by GOMETRAN. Because this inversion problem is underconstrained, an optimal estimation approach [*Rodgers*, 1976] was chosen that combines the information from the measurement with a priori information from a climatological database [*Fortuin and Kelder*, 1998] and an information matrix approach [*Kozlov*, 1983; *Hoogen et al.*, 1999a, 1999b]: By developing the difference between the iterative solution of the atmospheric state vector (including the ozone profile) to the a priori state vector into a series of eigenvectors with truncation of higher-order terms, the information content contained in the GOME measurements can be reduced to a minimum number of parameters (here the expansion coefficients) to be fitted, resulting in a numerically stable retrieval scheme. Temperature and pressure profiles are taken from the United Kingdom Meteorological Office (UKMO) assimilated data set [*Swinbank and O'Neill*, 1994]. Information about the surface height and albedo are taken from a database (R. Guzzi, surface type and height database, private communication, 1993) that is a reclassification of a database compiled from ~100 sources [*Matthews*, 1985]. The cloud cover is calculated from the measurements of the broadband Polarization Measurement Device (PMD) of GOME [*Kurosu*, 1998]. From the fractional cloud cover an effective albedo is determined. Figure 5 of *Hoogen et al.* [1999a] shows the solution standard deviation in fractions of the a priori standard deviation and the contributions from measurement noise

of GOME FURM: Between 11 and 42 km the measurement considerably improves the knowledge compared to the a priori statistics. Below and above the height range the ratio tends toward 1, and the information gain from the measurements decreases.

[9] The optimal estimation scheme uses the wavelength region 290–345 nm to derive vertical ozone profiles. While total ozone is derived from channel 2 spectra (315–400 nm) with an integration time of 1.5 s leading to a surface coverage of 40 km × 320 km, the short-wave channel of GOME (channel 1a: 240–307 nm before June 1998, currently 240–283 nm) has an integration time of 12 s, leading to a surface area coverage of approximately 100 km × 960 km for a single radiance measurement. Since June 1998 the upper boundary of the long-integration channel has been moved to 283 nm. However, since the signal-to-noise ratio is rather poor between 283 nm and 300 nm, coadding of subsequent GOME pixels to 12 s is still required for profile retrieval. Channel 2 spectra are also coadded to 12 s in order to homogenize surface coverage in channels 1a and 2. The nominal ground pixel size for GOME ozone profiles is thus 100 km × 960 km.

[10] Although ozone number density is retrieved on 71 equidistant altitude levels from 0 to 71 km, the vertical resolution of the GOME profiles is, typically, 7–8 km between about 20 and 35 km, as estimated from the full width at half maximum (FWHM) of the averaging kernels. This increases above and below the region of the ozone number density maximum [*Hoogen et al.*, 1999a]. As a result of the lower wavelength limit set at 290 nm, the current version of FURM (5.0) is limited to solar zenith angles below 76°. At SZA larger than 76° the integration time increases to 60 s in GOME channel 1a. Longer integration time at larger SZA, however, leads to large variation in solar zenith angles across the covered surface area, so that average geometric information for the viewing geometry as used in the current retrieval is not sufficient. Because of the larger ground scene at SZA larger than 76°, the geophysical inhomogeneity increases tremendously, and therefore no ozone profiles are retrieved.

[11] FURM results have been compared with ozonesonde profiles, which were convolved with GOME averaging kernels to degrade the sonde vertical resolution to that of GOME [*Hoogen et al.*, 1999b]. For five northern midlatitude to high-latitude sonde stations the GOME ozone number density has a positive bias of ∼5% with a root-mean-square (RMS) error of ∼10% at 20-km altitude. Dynamical variability in the lower stratosphere over the annual cycle is well reproduced by the GOME measurements as compared with annual sonde measurements [*Hoogen et al.*, 1999a, 1999b]. Comparison with global data from the Halogen Occultation Experiment (HALOE) aboard UARS with collocated FURM ozone profile between 17- and 32-km altitude shows an agreement to within 10–20%, except at locations close to or within the ozone hole [*Bramstedt et al.*, 2002]. Recent validation of GOME FURM results to means of the ALOMAR ozone lidar in northern Norway showed agreement within 7% in the altitude range 15–30 km [*Hansen et al.*, 2003].

2.1.2. SAGE II

[12] SAGE II uses solar occultation to measure the attenuation of solar radiation at the Earth's limb between the satellite and the Sun due to scattering and absorption by different species [*McCormick*, 1987]. The transmittance measurements are inverted using the "onion-peeling" approach to yield 1-km vertical resolution ozone profiles with a horizontal resolution of ∼200 km [*Mauldin et al.*, 1985; *Chu et al.*, 1989].

[13] From SAGE II measurements, ozone number concentrations at the 0.60-μm wavelength channel are derived, with the focus of the measurements on the lower and middle stratosphere (15–60 km). The instrument and ozone validation are discussed by *Chu et al.* [1989], *Cunnold et al.* [1989, 1996], and *McCormick et al.* [1989]. The previous versions of SAGE II data (versions 5.96 and 6.0) are discussed extensively by *Stratospheric Processes and Their Role in Climate* (*SPARC*) [1998] and *Manney et al.* [2001], respectively. SAGE II data have recently been reprocessed using version 6.2 retrieval algorithms, which is the version used in this study. This version was improved by an adjustment to the aerosol clearing and by the correction of channels at 525 and 1020 nm for absorption by the oxygen dimer (information on SAGE II can be found at http://www-sage2.larc.nasa.gov). First validation of SAGE II ozone data version 6.1 against ozonesonde data shows an accuracy of the SAGE II ozone data from the tropopause region up to 50 km to within 5% [*Wang et al.*, 2002].

2.2. Comparison Methods

2.2.1. Data Sets

[14] Complete data sets from GOME and SAGE II for July 1996 to June 2000 were searched for coincident measurements. Before April 1996, no GOME ozone profiles could be calculated from the level 1 data, because channel 2 measurements covered only the last quarter of the nominal ground scene, such that large gaps in the across-track sequence occurred. A matching of ground coverage between channel 1a and channel 2 was consequently not possible during this period [*Burrows et al.*, 1999]. The comparison between both instruments could not be extended after June 2000 because SAGE II experienced a failure of its azimuth gimbal system. This was corrected and operation at a 50% duty cycle was re-established by November 2000 (SAGE II website: http://www-sage2.larc.nasa.gov). In addition, since 2000 the degradation of the GOME scan mirror deteriorates the retrieval of ozone profiles by the FURM method because the earthshine and Sun spectra, which are divided to obtain the reflectance spectra, degrade at a different rate and it is difficult to retain absolute calibrated spectra [*Bramstedt et al.*, 2003].

2.2.2. Time and Spatial Criteria for Collocations

[15] Ozone profiles from GOME and SAGE II data have been compared for the coincidence criteria that measurements took place on the same day and that the tangent point of SAGE II is within 160 km of the center of the nearest GOME ground pixel. This ensures that the SAGE II tangent point is within the GOME ground pixel. The SAGE II profiles were interpolated from the bottom of the SAGE measurement to an altitude of 70 km at an interval of 1 km to enable statistical analyses between the collocated measurements having different vertical resolutions. In addition, ozone subcolumns from 10 to 18 km, 18 to 25 km, and 25 to 32 km from measurements of both instruments have

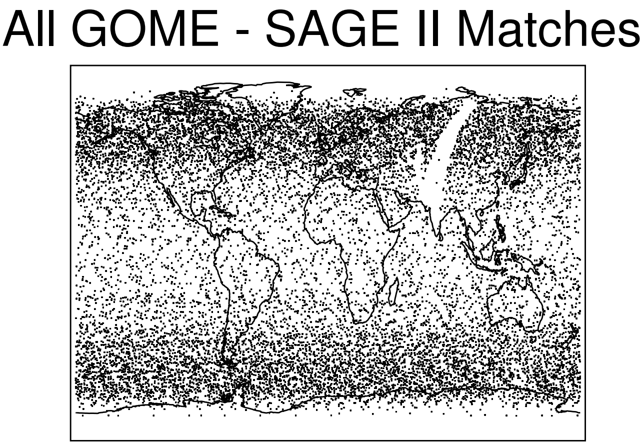

Figure 1. Location of all collocated GOME and SAGE II ozone measurements within a collocation radius of 160 km from July 1996 to June 2000.

been calculated and compared. The subcolumn altitude range roughly corresponds to the number of independent information in the retrieved vertical GOME profile. The data set of all coincident measurements was divided into subsets of four zonal bands in each hemisphere: high latitudes (60°–90°), midlatitudes (30°–60°), subtropics (15°–30°), and tropics (0°–15°).

2.2.3. Comparison Method of Matches Within Same Air Masses

[16] In order to avoid matches where the samples originate from different air masses, all coincident measurements were checked for their potential vorticity (PV) to identify air masses. PV values from the same day of each collocated measurement were taken from the United Kingdom Meteorological Office (UKMO) assimilated meteorological data set available in a 3.75° × 2.5° (longitude-latitude) grid resolution [*Swinbank and O'Neill*, 1994] and interpolated spatially to the observation point. Because of the quite large pixel size of a GOME profile with 960 × 100 km, the corner coordinates of each GOME profile were checked for the homogeneity of PV. For the SAGE II profile only the PV values at the tangent point were looked at, because the line of sight along the tangent point of a SAGE II ozone measurement is below 300 km [*Mauldin et al.*, 1985] and smaller than the UKMO data grid resolution. For samples outside the tropics, the tropopause height was determined with 3.5 PVU, which was proven by *Hoerling et al.* [1991] to be a good estimate for the dynamical tropopause height. Inside the tropics the smaller altitude of the 380-K isentropic level and 3.5-PVU level was selected for the tropopause. To consider only collocations where both GOME and SAGE II were inside the polar vortex or outside the vortex, matches have been included where both measurements were either greater than 40 or less than −40 PVU at 475 K (inside the vortex) or between −30 and 30 PVU at 475 K (outside the vortex), respectively. For the tropopause height, deviations within 1 km for collocations were tolerated.

2.2.4. Statistical Analysis of Collocated Measurements

[17] For each collocation pair the relative deviation RD between GOME and SAGE II ozone concentrations was determined at each altitude level h using equation (1):

$$\mathrm{RD}(h) = \frac{\mathrm{SAGE}[\mathrm{O_3}]_h - \mathrm{GOME}[\mathrm{O_3}]_h}{\left(\mathrm{SAGE}[\mathrm{O_3}]_h + \mathrm{GOME}[\mathrm{O_3}]_h\right) \times 0.5}. \quad (1)$$

[18] For each subset at each altitude level the mean relative deviation (MRD) and root-mean-square (RMS) of the relative deviation between all GOME and SAGE pairs were determined. For each subset, mean profiles and subcolumns for both instruments were calculated. Both instruments have a few measurements (<1%) with highly oscillating values that were removed from the statistical analyses by setting a criterion that only collocations be included where both measurements at 20-km altitude ($[\mathrm{O_3}]_{20\mathrm{km}}$) were within the following range (equation (2)):

$$\mathrm{MRD}_{20\,\mathrm{km}} - 4 \times \mathrm{RMS}_{20\,\mathrm{km}} \leq [\mathrm{O_3}]_{20\,\mathrm{km}} \leq \mathrm{MRD}_{20\,\mathrm{km}} + 4 \times \mathrm{RMS}_{20\,\mathrm{km}}. \quad (2)$$

3. Validation of GOME Ozone Profiles

[19] Over the 4-year time period from July 1996 to June 2000, 15,655 collocated GOME and SAGE II ozone measurements have been found (Figure 1 and Table 1). The matches are globally distributed from around 80°N to 80°S with most matches between 40° and 70°. There is only a swath stretching from Siberia to India where no collocations have been found. Here, descoping during the GOME operation takes place between two dump stations,

Table 1. Statistical Results of the Comparison of SAGE and GOME Ozone Profiles in Different Latitudinal Zones: Number of Collocations N, Altitude Range Where the Mean Relative Deviation is Less Than 10% and the Root-Mean-Square of the Mean Relative Deviation at These Altitudes Both Without Considering and Considering Atmospheric Dynamics Selection Criteria[a]

Zone	N Without ADSC	N With ADSC	MRD < 10% Without ADSC	MRD < 10% With ADSC	RMS Without ADSC	RMS With ADSC
60°–90°S	2376	806	18–20, 24–35 km	16–40 km	13–27%	10–15%
30°–60°S	4033	1507	19–35 km	18.5–35 km	12–18%	10–15%
15°–30°S	800	584	20–33 km	20–33 km	12–18%	10–15%
0° to 15°S	564	558	19.5–32 km	19.5–33 km	8–18%	8–15%
15°N to 0°	498	494	19.5–34 km	19.5–34 km	5–17%	5–15%
30°–15°N	750	532	19.5–32 km	19.5–33 km	5–18%	5–15%
60°–30°N	4181	1354	16–34 km	16–34 km	10–25%	10–20%
90°–60°N	2452	927	15–35.5 km	15–36 km	10–20%	10–15%
90°S to 90°N	15655	6762	18.5–34.5 km	18.5–34.5 km	10–25%	10–15%

[a]In this selection, no vertical resolution degradation was applied to SAGE II. ADSC, atmospheric dynamics selection criteria; MRD, mean relative deviation; RMS, root-mean-square.

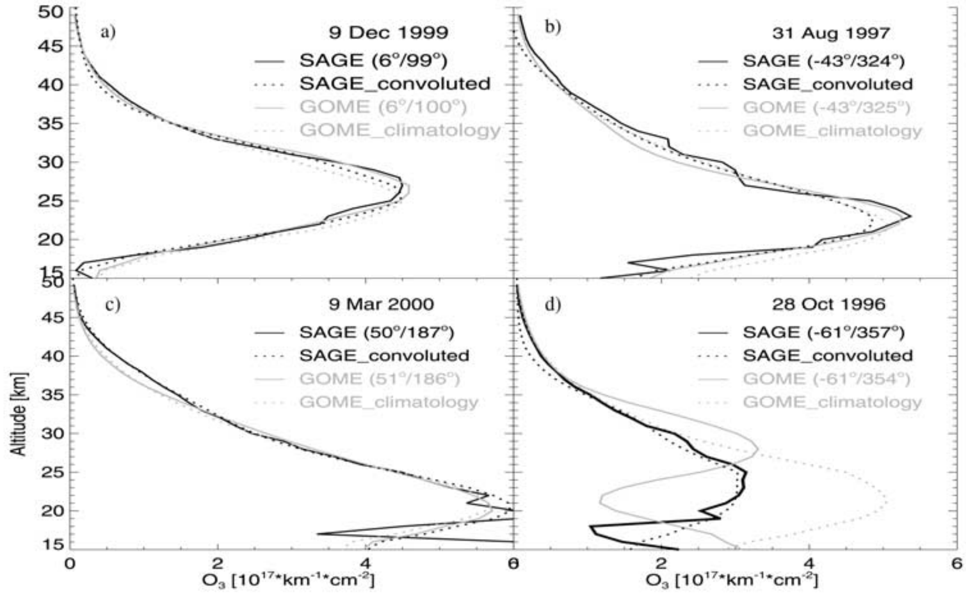

Figure 2. Examples of collocated ozone profiles from GOME (gray lines) FURM retrieval (solid lines) and a priori information (dotted lines) and SAGE II measurements (black lines) in original height resolution (solid lines) and convoluted with the GOME averaging kernels (dotted lines): (a) in the tropics, (b) in the southern midlatitudes, (c) in the northern midlatitudes, and (d) in the southern polar region.

which is a planned gap in data recording of GOME operations because of the limited capacity of the tape recorder. Looking only at collocations where the whole GOME pixel and the SAGE II pixel were in the same air mass regarding their tropopause height and their PV value at 475 K, 6762 matches were found (Table 1). Few matches from the low latitudes to 40° latitude were excluded, but more than 50% were excluded between the 40° and 70° latitudes in each hemisphere, because of large ozone gradients associated with tropopause height variability and polar vortex [e.g., *Weber et al.*, 2002].

[20] A few examples of collocated GOME and SAGE II ozone profiles are shown in Figure 2. The examples from the tropics (Figure 2a) and southern midlatitudes (Figure 2b) show good agreement between 18- and 50-km altitude. The example from around 50°N (Figure 2c) cannot resolve the double ozone peak between 19 and 23 km, as observed by SAGE II. This is explained by the coarse vertical resolution of the GOME profiles. Below 18 km, GOME deviates more strongly from SAGE II. That may be either due to clouds disturbing the SAGE II signal or due to the fact that for GOME FURM the information at these altitudes is nearly completely coming from the a priori profile. In addition to this, the asymmetric GOME averaging kernel alters the observed vertical ozone gradient below the ozone maximum peak [*Hoogen et al.*, 1999a], which can be also seen at higher values at these altitudes in the SAGE II profiles convolved with GOME averaging kernels compared to the ones at their original resolution. Figure 2d shows an example from October 1996 at high southern latitude where the GOME ozone profile was partly within and partly outside the vortex and the SAGE II ozone profile was measured inside the vortex. Therefore it is necessary to exclude such collocations from further statistical analyses by considering atmospheric dynamics criteria: The GOME PV values for this example ranged from −20 to −65 PVU, and the SAGE II PV value was around 50 PVU.

[21] Statistics over the comparison of all available GOME-SAGE collocated ozone measurements at each altitude level show good results with a mean relative deviation between 19 and 33 km of ±5% and a RMS of the mean relative deviation of 10–25% (Figure 3a and Table 1).

[22] Table 1 shows, for different zonal bands, the statistical results of all matches both without taking and taking both the tropopause height and the vortex edge criteria into consideration. For all collocations regardless of dynamical criteria, GOME and SAGE II show good agreement between 19 and 33 km (mean relative deviation of ±10% with RMS of 10–20%) in all zonal bands except at high southern latitudes. This can also be seen in the statistical results by comparing subcolumns (Table 2): For subcolumns the mean relative deviation of GOME to SAGE II ranges, at 18–25 km, between 0% and +8% bias with an RMS of 9–16%, and it ranges below 5% with an RMS of 4–12% at 25–32 km. At northern latitudes between 30° and 90° there is a good agreement down to 15 km. At high southern latitudes below 24 km (Figure 3b) the larger deviations between the two data sets probably result from matches where collocations are not homogenously within or outside the polar vortex. While the statistical results for all collocations where the matches were both within the same air mass (Figure 3c) appear similar for the mean relative deviation over all matches without using atmospheric dynamics criteria, the zonal statistics elucidate the fact that within the high southern latitudes this method improves the statistical result significantly (Tables 1 and 2 and Figure 3d): Here, the mean relative deviation is within 6% for the subcolumns between 18 and 32 km and 10% from 16 to 40 km for the height-resolved statistics. Also, the RMS is

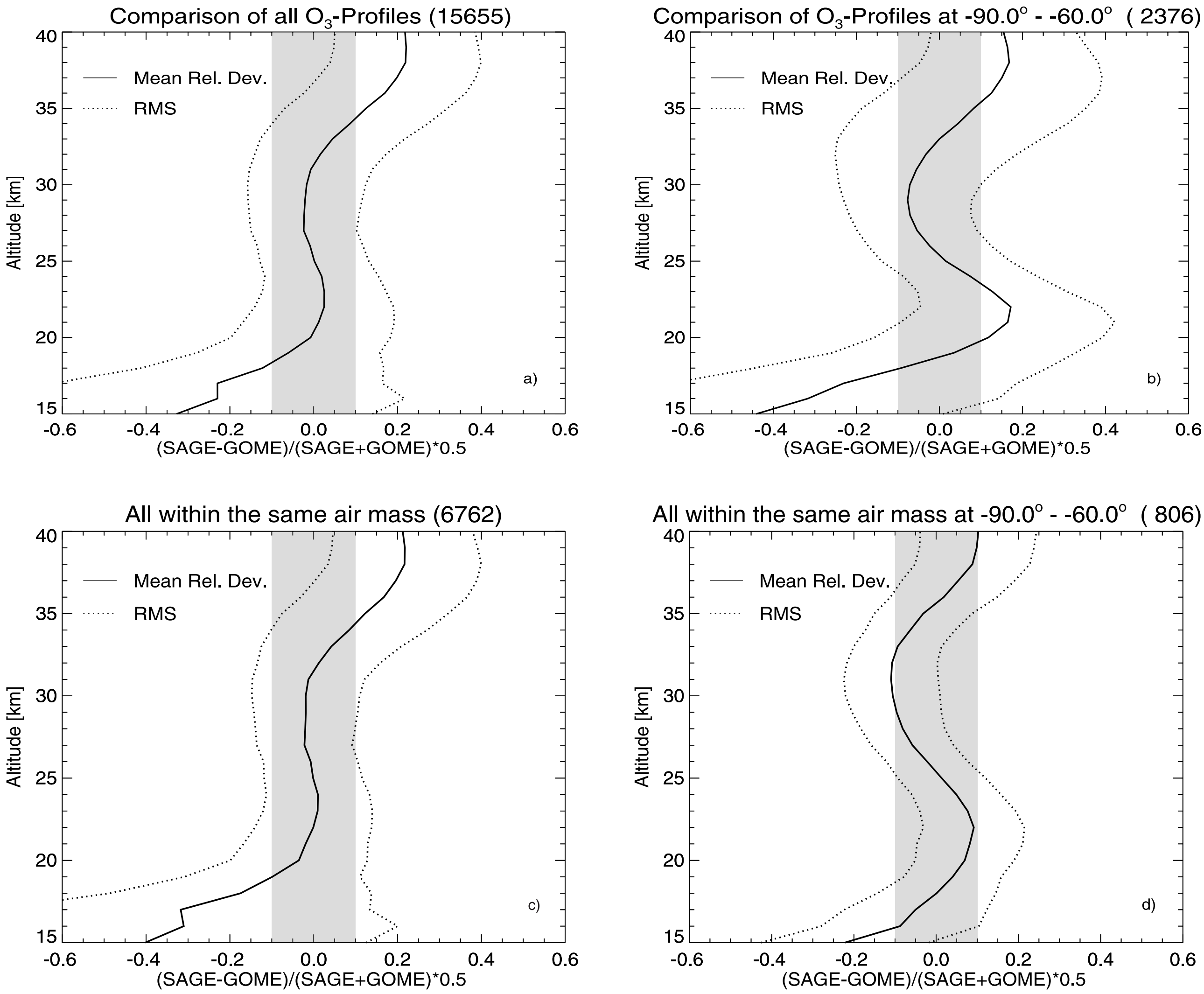

Figure 3. Mean relative deviation (solid lines) and the standard deviation (dotted lines) of the mean relative deviation of collocated GOME ozone profiles to SAGE II measurements: considering (a) all matches, (b) all matches between 60°S and 90°S, (c) only matches within the same air mass, and (d) only matches between 60°S and 90°S that are in the same air mass.

improved from 12–16% to 8% for the 18–32 subcolumns (Table 2) and from 27–13% to 10–15% for the height-resolved comparison (Table 1). However, in addition to this, the inclusion of collocated measurements, where both are within the same air mass, improves the RMS between 18 and 32 km in all zonal bands as compared to the comparison of all collocated measurements by 2–5%. One has to bear in mind that the number of coincidences in these statistical

Table 2. Mean Relative Deviation and the Root-Mean-Square of the Mean Relative Deviation, Calculated With Equation (1), of the Comparison of GOME FURM and SAGE II Ozone Profiles in Different Latitudinal Zones Within the Three Subcolumns 10–18 km, 18–25 km, and 25–32 km Both Without Considering and Considering Atmospheric Dynamics Selection Criteria[a]

Zone	10–18 km Without ADSC	10–18 km With ADSC	18–25 km Without ADSC	18–25 km With ADSC	25–32 km Without ADSC	25–32 km With ADSC
60°–90°S	−24% ± 20%	−15 ± 10%	10% ± 16%	6% ± 8%	−5% ± 12%	−5% ± 8%
30°–60°S	−24% ± 26%	−26% ± 27%	0% ± 11%	0% ± 10%	2% ± 10%	2% ± 9%
15°–30°S	−55% ± 40%	−60% ± 40%	−8% ± 10%	−8% ± 10%	1% ± 10%	0% ± 10%
0° to 15°S	−84% ± 42%	−84% ± 43%	−6% ± 11%	−6% ± 10%	−3% ± 7%	−3% ± 7%
15°N to 0°	−90% ± 40%	−91% ± 40%	−2% ± 10%	−2% ± 10%	−4% ± 4%	−4% ± 4%
30°N to 15°N	−53% ± 41%	−61% ± 40%	−7% ± 8%	−7% ± 7%	−2% ± 5%	−2% ± 4%
60°–30°N	−13% ± 26%	−15% ± 27%	−2% ± 9%	−2% ± 9%	−1% ± 9%	0% ± 8%
90°–60°N	−8% ± 16%	−6% ± 14%	0% ± 9%	−1% ± 7%	−3% ± 9%	−3% ± 8%
90°S to 90°N	−29% ± 34%	−31% ± 41%	0% ± 12%	−2% ± 9%	−1% ± 10%	−1% ± 8%

[a]ADSC, atmospheric dynamics selection criteria.

Table 3. Mean Relative Deviation and the Root-Mean-Square of the Mean Relative Deviation, Calculated With Equation (1), of the Comparison of GOME A Priori and SAGE II Ozone Profiles in Different Latitudinal Zones Within the Three Subcolumns 10–18 km, 18–25 km, and 25–32 km Both Without Considering and Considering Dynamical Aspects[a]

Zone	10–18 km Without DA	10–18 km With DA	18–25 km Without DA	18–25 km With DA	25–32 km Without DA	25–32 km With DA
60°–90°S	−31% ± 40%	−6 ± 16%	−14% ± 30%	−2% ± 21%	−9% ± 16%	−5% ± 13%
30°–60°S	−13% ± 13%	−16% ± 37%	−3% ± 11%	3% ± 10%	−4% ± 13%	−3% ± 12%
15°–30°S	−55% ± 43%	−63% ± 42%	−8% ± 10%	−8% ± 10%	4% ± 9%	5% ± 9%
0° to 15°S	−89% ± 43%	−90% ± 44%	−7% ± 10%	−7% ± 10%	8% ± 6%	8% ± 6%
15°N to 0°	−100% ± 40%	−100% ± 40%	−10% ± 10%	−10% ± 10%	7% ± 4%	7% ± 4%
30°–15°N	−55% ± 46%	−64% ± 44%	−7% ± 9%	−7% ± 8%	5% ± 6%	6% ± 6%
60°–30°N	−8% ± 38%	−8% ± 42%	−2% ± 11%	−2% ± 11%	−1% ± 10%	−1% ± 10%
90°–60°N	−8% ± 23%	−5% ± 22%	−1% ± 9%	−1% ± 9%	−2% ± 13%	2% ± 12%
90°S to 90°N	−24% ± 44%	−31% ± 50%	−6% ± 15%	−4% ± 14%	−1% ± 12%	2% ± 10%

[a]DA, dynamical aspects.

analyses may influence the RMS values. If the number of coincidences with atmospheric dynamics criteria were the same as without the criteria, the RMS of the statistics over all coincidences within the same air mass would be even lower.

[23] As expected, overall the subcolumn-based statistics of SAGE II and GOME are in even better agreement than the altitude-resolved statistics, because the first takes into account the lower vertical resolution of the GOME profiles. However, regardless of the collocation criteria used, both comparisons show that below 18 km, GOME is generally higher than SAGE II and exhibits a very high RMS up to 45%.

[24] Table 3 shows the results of comparisons of GOME a priori profiles with SAGE II for the three subcolumn altitude ranges. This comparison was made in order to check whether the observed improvement in GOME/SAGE comparisons when dynamical effects are accounted for is partially due to selectively removing cases where the GOME a priori profile is significantly different from the true ozone profile. Results show that for all three subcolumns, except for the zone between 60°S and 90°S, the mean relative deviation and the RMS between the GOME a priori and SAGE II profiles did not improve after applying the dynamical criteria as in the comparisons between GOME FURM and SAGE II: No change was seen for the two upper subcolumns between 18 and 32 km, but an increase was seen in both mean relative deviation and its RMS for the 10–18-km subcolumn. One can conclude that for the tropopause height criterion the GOME a priori profile is not affecting the improvements found for including dynamical aspects, but when filtering for the polar vortex, the a priori information is also improving significantly the comparability of FURM profiles to SAGE II.

4. Long-Term Trends in Ozone Subcolumns of GOME and SAGE

[25] The time series of all collocated SAGE II and GOME ozone subcolumns from 10 to 18 km, 18 to 25 km, and 25 to 32 km in different zonal bands are shown in Figures 4a, 4b, and 4c. Except for high latitudes (60°–90°), collocations between SAGE II and GOME were found for nearly all months.

[26] The 10–18-km (Figure 4a) ozone subcolumns are highest in the middle to high latitudes and decrease with decreasing latitude. SAGE II and GOME ozone subcolumns in all latitudinal bands follow each other, but nearly everywhere GOME mean values are higher than or at least equal to SAGE II values. At midlatitudes (30°–60°) the annual cycle in ozone subcolumns with maxima during late winter–early spring is observed. This is more pronounced in the Northern Hemisphere; a similar pattern is observed in Arctic latitudes (maxima in spring), but in Antarctic latitudes, spring ozone values are about the same as or even lower than those during other times of the year, indicating strong chemical ozone depletion. For both middle and high latitudes, SAGE II and GOME mean values in the Northern Hemisphere are very close to each other, while in the Southern Hemisphere, discrepancies are bigger between mean values of both instruments.

[27] SAGE II and GOME ozone subcolumns between 18 and 25 km (Figure 4b) follow each other in all latitudinal bands except for the high southern latitudes, where deviations between the mean and RMS values are larger. Ozone subcolumn values are highest between 30° and 90° and then decrease with decreasing latitude. In the subtropics and tropics (between 30°S and 30°N), GOME ozone subcolumns are higher than or about the same as SAGE II values. However, in the northern tropics and middle and high latitudes, sometimes SAGE mean values are higher. The tropical ozone values measured by both instruments show a minimum in January 1998 of 60–65 DU (depending on the instrument used for measuring and on the hemisphere). In the southern subtropics an annual cycle in the ozone subcolumn is detected with maxima during winter (July to September), but not in the equivalent latitudes of the Northern Hemisphere. Also at midlatiudes (30°–60°), an annual cycle in the 18–25-km subcolumns with maximal values during winter can be observed. This annual pattern is also pronounced at high northern latitudes, with maxima in spring, but in the high southern latitudes the ozone values in spring range from maximal values over 140 DU to minimal values below 40 DU, indicating that collocations are as good inside as outside the polar vortex. In accordance with this, the large deviations between the mean and RMS ozone subcolumn values of SAGE II and GOME mainly during late winter and spring in this zonal band correspond to the fact that at quite a few collocations both collocated measurements were not either completely inside or outside the polar vortex.

[28] Subcolumns between 25 and 32 km from SAGE II and GOME ozone follow each other in all latitudinal bands

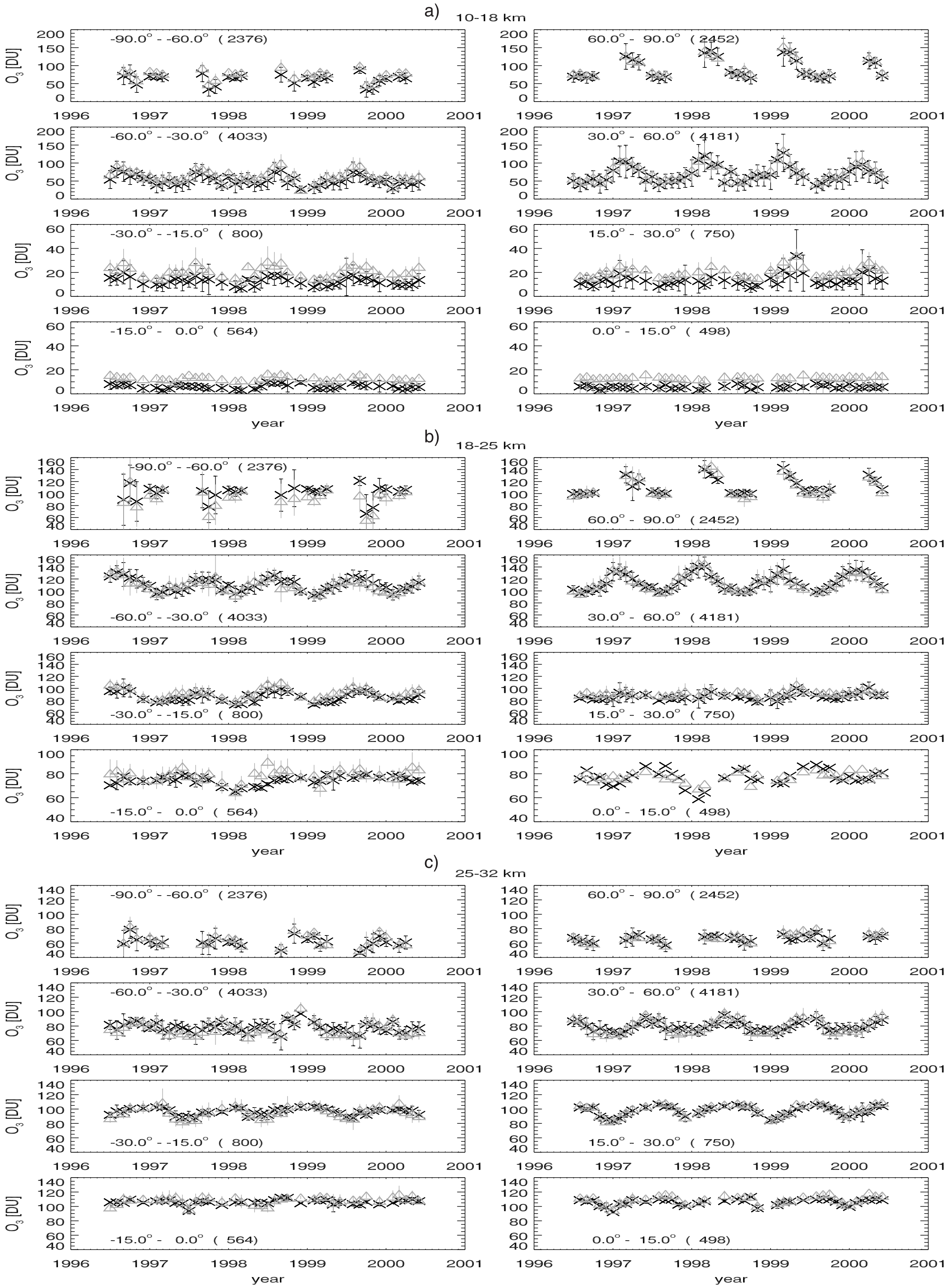

Figure 4. Mean ozone subcolumns of all collocated GOME and SAGE II ozone measurements at (a) 10–18 km, (b) 18–25 km, and (c) 25–32 km calculated for different latitudinal zones.

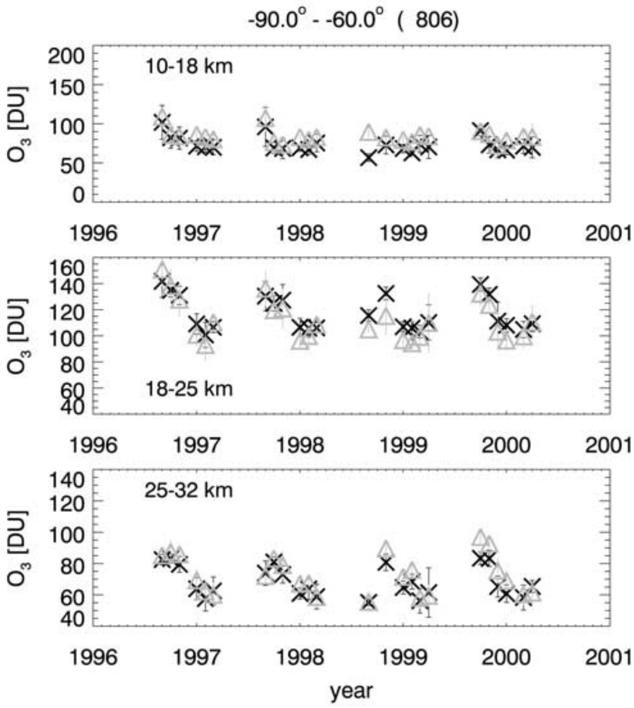

Figure 5. Mean ozone subcolumns calculated from all collocated GOME and SAGE II ozone measurements at 60°–90°S within the same air mass at 10–18 km, 18–25 km, and 25–32 km.

(Figure 4c). Overall, in the Northern Hemisphere, deviations between the mean and RMS subcolumns of SAGE II and GOME are smaller than at southern latitudes. In the tropics and in the southern high latitudes, GOME ozone subcolumns are higher than or about the same as SAGE II values as opposed to the other latitudinal subsets, where SAGE mean values can also be higher than GOME. Ozone subcolumn values are highest in the low latitudes and decrease with increasing latitude. An annual cycle in the ozone subcolumn with minimum values during the winter can be seen in all latitudinal subsets: very weak, as expected, in the tropics; clearly visible in the subtropics and midlatitudes but here less pronounced in the Southern Hemisphere; and also weak in the high latitudes, where, because of no light in winter, these values are missing.

[29] The time series of all collocated SAGE II and GOME ozone subcolumns from 10 to 18 km, 18 to 25 km, and 25 to 32 km where both matches were in the same air mass showed no differences from the analyses using all collocations shown in Figure 4, except for high southern latitudes, where significant improvements are observed (Figure 5). Differences are most pronounced in the 18–25-km subcolumns, where the deviations between GOME and SAGE II mean values become much smaller. Since all collocations considering dynamical aspects were outside the polar vortex, subcolumn values are not below 80 DU, as opposed to values of <40 DU where all collocations in this subset were considered. The trend can also be seen at 10–18 km with smaller deviations between the mean subcolumns of GOME and SAGE II and lowest values around 60 DU, as opposed to values down to 10 DU considering all matches. For subcolumns between 25 and 32 km, deviations among collocations within the same air mass are about the same as deviations considering all collocations, but the RMS of the values is decreased significantly.

5. Summary and Conclusions

[30] The overall agreement between ozone profiles from GOME FURM (version 5.0) and SAGE II (version 6.2) is remarkably good between 19 and 35 km. When atmospheric dynamics criteria are considered, good agreement extends down to 16 km in the middle to high latitudes.

[31] The tropospheric ozone subcolumn represents less than 10% of the total ozone column, which makes the retrieval of reliable profile information from GOME nadir spectra challenging and requires excellent radiometric calibration. The asymmetric GOME averaging kernel, which alters the observed vertical ozone gradient below the ozone maximum peak [*Hoogen et al.*, 1999a], may explain why GOME ozone subcolumns between 10 and 18 km are generally always higher than those of SAGE II. This means that some contribution of the lowermost stratosphere is smoothed into the tropospheric column. In the lowermost stratosphere, occultation instruments may suffer from enhanced aerosol and high solar extinction, which also increase the SAGE retrieval error. Above 35 km, information on stratospheric ozone has to be extracted from GOME measurements at shorter wavelengths (<290 nm). Careful selection of the wavelength has to be made to avoid emission features from the upper atmosphere from metals and NO_y gamma bands. The spectral residuals are getting larger below 290 nm as a result from the inadequate radiometric calibration of the instrument at these wave-

Table 4. Months Where Ozone Minima and Maxima of the Annual Cycles Are Observed (in Figures 4a–4c and 5) in SAGE II and GOME Subcolumn Measurements From July 1996 to June 2000[a]

	Minima			Maxima		
Subcolumn	10–18 km	18–25 km	25–32 km	10–18 km	18–25 km	25–32 km
60°–90°S	–	–	Sept.[b]	Sept.[b]	–	Oct.–Dec.[b]
30°–60°S	Dec.–Feb.	Feb.	–	Aug.–Sept.	Aug.	–
15°–30°S	Feb.–March	Feb.	July–Aug.[b]	Aug.–Sept.[b]	Aug.–Sept.	Feb.–March
0° to 15°S	–	–	–	–	–	–
15°N to 0°	–	–	Nov.–Jan.[b]	–	–	Sept.–Oct.[b]
30°–15°N	Aug.–Sept.[b]	Sept.–Oct.[b]	Dec.–Jan.	Feb.–May[b]	Feb.–May[b]	July–Aug.
60°–30°N	Aug.	Aug.	Dec.–Feb.	March	Feb.–March	June–July
90°–60°N	July–Sept.	July–Sept.	–	March	March–April	–

[a]Dashes indicate no annual cycle.
[b]Only weak expression of annual cycle.

lengths [*Tellmann et al.*, 2004]. With the current limitation of the usable wavelength range to above 290 nm the altitude range where sensible ozone values can be retrieved from GOME is limited. Additional calibration corrections are currently underway that may enable to extend the retrieval to the upper stratosphere. This is expected to improve the retrieval of ozone profiles from GOME in the tropics significantly, but also at latitudes outside the tropics, ozone retrieval being now reasonable from the tropopause to around 50 km.

[32] Analysis of the results of our study provides quantitative comparisons of GOME ozone profiles with independent measurements having a higher vertical resolution. This shows that the optimal comparisons are achieved using subcolumns for an altitude range matching the GOME vertical resolution. This study also showed that it is important when collocated measurements for ozone comparisons are selected to also consider the homogeneity of volume air sampled by GOME and SAGE II. The PV value at the 475-K isentrope was used for this purpose to distinguish polar vortex air masses from others. When in addition the homogeneity of the tropopause height was required, improvement was found by lowering the RMS of the mean relative deviation by ~2% when comparing subcolumns and by ~2–5% for the height-resolved comparison. The altitude range at which the GOME ozone profiles are within 10% of the SAGE II profiles extended by ~1 km at the upper and lower ends. For comparisons of multiplatform measurements where only a small number of matches have been found within a chosen spatial-temporal vicinity, *Danilin et al.* [2002] used a method enlarging the amount of matching by using a trajectory-hunting technique. The results showed that in this case with the trajectory-hunting technique, comparisons were statistically more robust than just limiting the comparisons to the traditional correlative analysis. Our study shows that analysis of a large data set for zonal mean comparisons including atmospheric dynamics criteria for the selection of collocated measurements slightly improves the statistics, but for individual comparisons the criteria used result in significant improvement.

[33] The time series of the comparisons of ozone profiles retrieved from GOME and SAGE II measurements (Figures 4 and 5) show, for all three subcolumns, annual cycles in all latitudinal zones, including a weak cycle at low latitudes (summarized in Table 4). At the northern midlatitudes the annual cycle of ozone is more pronounced than it is at the southern midlatitudes. This results from the stronger role of planetary wave activity in this hemisphere, leading to higher ozone maxima than in the Southern Hemisphere [*Weber et al.*, 2003]. The maximum and minimum values in both hemispheres coincide during the same time period for both subcolumns 10–18 km and 18–25 km. However, for the 25–32-km subcolumns at all latitudinal zones, the values are vice versa: The maximum values appear during times when lower altitude subcolumns show minimum values, and the minimum values appear during times when the lower altitude subcolumns show maximum values (Table 4).

[34] From these results we conclude that the GOME nadir sensor already provides a valuable global data set of ozone vertical distribution using a restricted set of wavelengths. Improvements for GOME ozone profiles are expected to be obtained from the soon to be released new FURM version 6.0, in which the analysis of wavelengths shorter than 290 nm will also be included.

[35] **Acknowledgments.** This work is funded in part by DLR-Bonn (contract 50 EE0025) and BMBF (FKZ 01 SF9994). We would like to thank DLR-Oberpfaffenhofen for providing GOME calibrated level 1 spectral data version 2.0. We thank the SAGE II group at NASA LaRC, especially Larry Thomason, and the NASA Langley Radiation and Aerosols Branch for providing us with data from this instrument and information about the data and instrument and the DLR/DFD-Oberpfaffenhofen for providing GOME spectral data.

References

Bramstedt, K., K.-U. Eichmann, M. Weber, V. Rozanov, and J. P. Burrows (2002), GOME ozone profiles: A global validation with HALOE measurements, *Adv. Space Res.*, *29*(11), 1637–1642.

Bramstedt, K., J. Gleason, D. Loyola, W. Thomas, A. Bracher, M. Weber, and J. P. Burrows (2003), Comparison of total ozone values from the satellite instruments GOME and TOMS with measurements from the Dobson network 1996–2000, *Atmos. Chem. Phys.*, *3*, 1409–1419.

Burrows, J. P., et al. (1999), The Global Ozone Monitoring Experiment (GOME): Mission concept and first scientific results, *J. Atmos. Sci.*, *56*, 151–175.

Chu, W. P., M. P. McCormick, J. Lenoble, C. Brogniez, and P. Pruvost (1989), SAGE II inversion algorithm, *J. Geophys. Res.*, *94*, 8339–8351.

Cunnold, D. M., W. P. Chu, R. A. Barnes, M. P. McCormick, and R. E. Veiga (1989), Validation of SAGE II ozone measurements, *J. Geophys. Res.*, *94*, 8447–8460.

Cunnold, D. M., H. Wang, W. P. Chu, and L. Froidevaux (1996), Comparisons between Stratospheric Aerosol and Gas Experiment II and Microwave Limb Sounder ozone measurements and aliasing SAGE II ozone trends in the lower stratosphere, *J. Geophys. Res.*, *101*, 10,061–10,075.

Danilin, M. Y., et al. (2002), Comparison of ER-2 aircraft and POAM III, MLS, and SAGE II satellite measurements during SOLVE using traditional correlative analysis and trajectory hunting technique, *J. Geophys. Res.*, *107*, 8315, doi:10.1029/2001JD000781. [printed *108*(D5), 2003]

de Beek, R., R. Hoogen, V. V. Rozanov, and J. P. Burrows (1997), Ozone profile retrieval from GOME satellite data I: Algorithm description, *Eur. Space Agency Spec. Publ., ESA-SP414*, 749–754.

Eichmann, K.-U. (2001), Die Ozonverteilungen der Nordhemisphere 1997–2000 gemessen mit GOME: Einfluss von Dynamik und Chemie in der Stratosphäre, Ph.D. thesis, 182 pp., Univ. of Bremen, Bremen, Germany.

Eichmann, K.-U., K. Bramstedt, M. Weber, R. Hoogen, V. Rozanov, and J. P. Burrows (1999), Structure of ozone mini-holes from GOME, in *European Symposium on Atmospheric Measurements From Space*, *ESA-WPP-161*, pp. 231–236, Eur. Space Res. and Technol. Cent., Eur. Space Agency, Nordwijk, Netherlands.

Eichmann, K.-U., K. Bramstedt, M. Weber, V. Rozanov, and J. P. Burrows (2000), The structure of ozone mini-holes from GOME satellite observations, in *Stratospheric Ozone 1999: Proceedings of the Fifth European Symposium on Stratospheric Ozone Research*, *EC Air Pollut. Res. Rep.*, vol. 73, pp. 483–486, Saint Jean de Luz, France.

Fishman, J., V. Ramanathan, P. J. Crutzen, and S. C. Liu (1979), Tropospheric ozone and climate, *Nature*, *282*, 818–820.

Fortuin, J. P. F., and H. M. Kelder (1998), An ozone climatology based on ozone sondes and satellite measurements, *J. Geophys. Res.*, *103*, 31,709–31,719.

Hansen, G., K. Bramstedt, V. Rozanov, M. Weber, and J. P. Burrows (2003), Validation of GOME ozone profiles with ALOMAR ozone lidar, *Ann. Geophys.*, *21*, 1879–1886.

Hoerling, M. P., T. K. Schaak, and A. J. Lenzen (1991), Global objective tropopause analyses, *Mon. Weather Rev.*, *119*, 1816–1831.

Hoogen, R., V. V. Rozanov, and J. P. Burrows (1999a), Ozone profiles from GOME satellite data: Algorithm description and first validation, *J. Geophys. Res.*, *104*, 8263–8280.

Hoogen, R., V. V. Rozanov, K. Bramstedt, K.-U. Eichmann, M. Weber, and J. P. Burrows (1999b), Ozone profiles from GOME satellite data I: Comparison with ozone sondes measurements, *Phys. Chem. Earth, Part C: Sol.-Terr. Planet. Sci.*, *24*, 447–452.

James, P. M. (1998), A climatology of ozone mini-holes over the Northern Hemisphere, *Int. J. Climatol.*, *18*, 1287–1303.

Kozlov, V. (1983), Design of experiments related to the inverse problem of mathematical physics (in Russian), in *Mathematical Theory of Experiment Design*, edited by C. M. Ermakov, pp. 216–246, Nauka, Moscow.

Kurosu, T. (1998), PMD cloud detection algorithm for the GOME instrument: Algorithm description and users manual, *Tech. Rep. 11,572/2/95/*

NL/CN, Eur. Space Res. and Technol. Cent., Eur. Space Agency, Nordwijk, Netherlands.
Manney, G. L., et al. (2001), Comparison of satellite ozone observations in coincident air masses in early November 1994, *J. Geophys. Res.*, *106*, 9923–9943.
Matthews, E. (1985), Atlas of archived vegetation, land-use and seasonal albedo data sets, *NSA Tech. Memo. 86199*, Natl. Oceanic and Atmos. Admin., Boulder, Colo.
Mauldin, L. E., III, N. H. Zuan, M. P. McCormick, J. H. Guy, and W. R. Vaughn (1985), Stratospheric Aerosol and Gas Experiment: A functional description, *Opt. Eng.*, *24*, 307–312.
McCormick, M. P. (1987), SAGE II: An overview, *Adv. Space Res.*, *7*(3), 219–226.
McCormick, M. P., J. M. Zawodny, R. E. Veiga, J. C. Larsen, and P. H. Wang (1989), An overview of SAGE I and SAGE II ozone measurements, *Planet. Space Sci.*, *37*, 1567–1586.
McKenna, D. S., R. L. Jones, J. Austin, E. V. Browell, M. P. McCormick, A. J. Krueger, and A. F. Tuck (1989), Diagnostic studies of the Antarctic vortex duirng the 1987 Antarctic ozone experiment: Ozone mini-holes, *J. Geophys. Res.*, *94*, 11,641–11,668.
Newman, P. A., L. R. Lait, and M. R. Schoeberl (1988), The morphology and meteorology of Southern Hemisphere spring total ozone mini-holes, *Geophys. Res. Lett.*, *15*, 923–926.
Ramanathan, V., and R. E. Dickinson (1979), The role of stratospheric ozone in the zonal and seasonal radiation energy balance of the Earth troposphere system, *J. Atmos. Sci.*, *36*, 1084–1104.
Ramanathan, V., L. B. Callis, and R. W. Boughner (1976), Sensitivity of surface temperature to perturbations in the stratospheric concentrations of ozone and nitrogen dioxide, *J. Atmos. Sci.*, *33*, 1092–1112.
Rodgers, C. D. (1976), Retrieval of atmospheric temperature and composition from remote measuremetns of thermal radiation, *Rev. Geophys.*, *14*, 609–624.
Rozanov, V. V., D. Diebel, R. J. D. Spurr, and J. P. Burrows (1997), GOMETRAN: A radiative transfer model for the satellite project GOME, The plane-parallel version, *J. Geophys. Res.*, *102*, 16,683–16,695.
Stratospheric Processes and Their Role in Climate (SPARC) (1998), Assessment of trends in the vertical distribution of ozone, *SPARC/IO3C/GAW*, World Meteorol. Organ. Global Ozone Res. and Monit. Proj., Geneva.
Swinbank, R., and A. O'Neill (1994), A stratosphere-troposphere data assimilation system, *Mon. Weather Rev.*, *122*, 686–702.
Tellmann, S., V. V. Rozanov, M. Weber, and J. P. Burrows (2004), Improvement in the tropical ozone profile retrieval from GOME-UV/VIS nadir spectra, *Adv. Space Res.*, *34*, 739–742.
Wang, H. J., D. M. Cunnold, L. W. Thomason, J. M. Zawodny, and G. E. Bodeker (2002), Assessment of SAGE version 6.1 ozone data quality, *J. Geophys. Res.*, *107*(D23), 4691, doi:10.1029/2002JD002418.
Wang, W.-C., Y.-C. Zhuang, and R. D. Bojkov (1993), Climate implications of observed changes in ozone vertical distributions at middle and high latitudes of the Northern Hemisphere, *Geophys. Res. Lett.*, *20*, 1567–1570.
Weber, M., K.-U. Eichmann, F. Wittrock, K. Bramstedt, L. Hild, A. Richter, J. P. Burrows, and R. Müller (2002), The cold winter 1995/1996 as observed by the Global Ozone Monitoring Experiment GOME and HALOE: Tropospheric wave activity and chemical ozone loss, *Q. J. R. Meteorol. Soc.*, *128*, 1293–1319.
Weber, M., S. Dhomse, F. Wittrock, A. Richter, B.-M. Sinnhuber, and J. P. Burrows (2003), Dynamical control of NH and SH winter/spring total ozone from GOME observations in 1995–2002, *Geophys. Res. Lett.*, *30*(11), 1583, doi:10.1029/2002GL016799.
Weiss, A. (2000), Anthropogenic and dynamic contributions to ozone trends of the Swiss total ozone, Umkehr and balloon sounding series, Ph.D. thesis, 159 pp., Swiss Fed. Inst. of Technol., Zürich.
Zellner, R., T. Peter, K. Dämmer, and L. Quitem (Eds.) (1999), *10 Jahre Deutsche Ozonforschung* (in German), Verl. für Market. und Kommun., Monsheim, Germany.

A. Bracher, K. Bramstedt, J. P. Burrows, S. Tellmann, and M. Weber, Institute of Environmental Physics, University of Bremen, P. O. Box 330440, Otto-Hahn-Allee 1, D-28334 Bremen, Germany. (bracher@uni-bremen.de)